THE RELATIONSHIP BETWEEN CONTINUOUS COOLING RATE AND MICROSTRUCTURE IN THE HEAT AFFECTED ZONE (HAZ) OF THE DISSIMILAR WELD BETWEEN CARBON STEEL AND AUSTENITIC STAINLESS STEEL

Le Thi Nhung[1)], Pham Mai Khanh[1)], Le Minh Hai[1)], Nguyen Duong Nam[2)]*
[1)] School of Materials Science and Engineering, Hanoi University of Science and Technology, Hanoi, Vietnam
[2)] School of Mechanical Engineering, Vietnam Maritime University, Hai Phong, Vietnam

Received: 04.10.2017
Accepted: 08.10.2017

[*]Corresponding author: e-mail: khanh.phammai@hust.edu.vn, Tel.: +84983030011, School of Materials Science and Engineering, Hanoi University of Science and Technology, 1 Dai Co Viet, Hai Ba Trung, Hanoi, Vietnam

Abstract
This paper investigates the changed in the microstructure in HAZ of the dissimilar weld between carbon steel and 304 austenitic stainless steel. Continuous cooling transformation diagrams (CCT), peak temperature profiles and cooling rates can be used to predict the change in the microstructure of the HAZ during the welding process. Optical microscopy, X – ray, SEM and TEM were used to determine the phases which formed in HAZ of carbon steel and austenitic stainless steel. The results of this study indicate that grain size in HAZ depended on the temperature at that point could be reached during the welding. Fully Martensitic layer observed at the interface in carbon side due to the combination of the rapid cooling subsequent to weld and local chemical composition. Cooling rate played the rule on forming Widmanstatten ferrite, Bainite and Pearlite. On the other hand, microstructures and grain size in HAZ of austenitic stainless steel were not affected by temperature and cooling rate. Carbides precipitation ($M_{23}C_6$, M_7C_3), however, were found in the boundary of grains.

Keywords: Dissimilar weld, microstructure, cooling rate, HAZ

1 Introduction

Mechanical properties of steels are strongly connected to their microstructure obtained after the welding process. It was found in previous studies that the microstructures of weldments were affected by composition, peak temperature and cooling rate [1-10]. Especially, cooling rate was an important variable which played a key role in phase transformation, microstructure as well as mechanical properties. In welding processes, as the cooling rate in the weld zone and heat affected zone (HAZ) varied with cooling distance from the fusion line of the weld, the phases formed from the transformation was observed to also vary with cooling distance [7]. For example with low carbon steel, increasing the cooling rate resulted in the gross microstructure changing from coarse, polygonal Ferrite to acicular Ferrite to upper Bainite. A blocky or elongated Martensitic – Austenite microconstituent was also observed [1, 2]. Cooling rate also significantly affected the formation of intermetallic phases and corrosion resistance and hot cracking in stainless steel [11-14]. Differences in the cooling rate appeared to provide dramatic effects on the microhardness of steels, depending on the carbon content of steels [5, 10, 15, 16]. The samples cooled with salty water had higher hardness values possibly due to the formation of

DOI 10.12776/ams.v23i4.1002 p-ISSN 1335-1532
e-ISSN 1338-1156

Martensitic after quenching, while air-cooled samples were mostly Ferrite [7]. The microhardness increased with the increasing cooling rate and carbon content due to solid solution hardening and formation of the Martensitic phase. Thus heat treatment (heating and cooling) was used to obtain desired properties of steels such as improving the toughness, ductility or removing the residual stresses [4].

In practice, the cooling rate depends on a number of variables, for example, heat input, process efficiency, preheat temperature, material properties and wire feeding rate. Rosenthal developed an equation for predicting cooling rates and peak temperatures in HAZ of weldment for thin plates. On the other hand, cooling rate and peak temperatures could be measured by thermocouple [17-21].

Because weld metals are subjected to continuous cooling upon solidification, the resultant microstructures should be predictable from continuous cooling transformation (CCT) diagrams [24-27]. Therefore, before presenting the results of the metallographic analysis, a brief summary of the type of weld metal microstructures can determine from CCT diagrams base on material compositions and cooling rates.

2 Experimental procedure

As received plates of carbon steel and 304 stainless steel were machined to dimensions of 275 x 85 x 3 mm, then edge joint preparation and cleaning were required before welding. The chemical composition of the base metal and filler are presented in **Table. 1**. The welding joints were made by shielded metal arc welding (SMAW). The welding parameters in the processes shown in **Table. 2**. Thermocouples (K – type) were used to measure the transient temperature distribution during welding. The position of thermocouples is shown in **Table. 3**.

Table 1 The chemical composition of the base metal and filler

Alloys	C	Mn	Si	S	P	Cr	Ni	Mo	V
304 stainless steel	0,09	1,54	0,49	0.005	0,005	18.3	7.56	0,13	0,11
Carbon steel	0,18	0,62	0,02	0,04	0,05	0,02	0,08	0.005	0,01
Filler E309L - 16	0,03	1.34	0,71	0.005	0.003	23.7	12.6	-	-

Table 2 The welding parameters

Parameters	I (A)	U (V)	V (mm/min)	Preheat (^{0}C)
Values	80	25	100	30

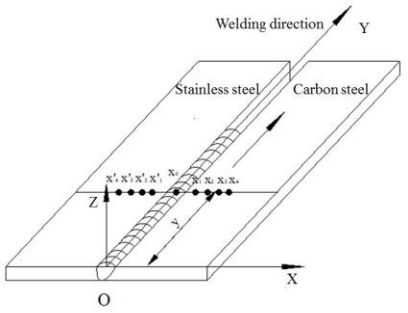

Table 3 The positions of thermocouple on the carbon steel and stainless steel plates

Positions	HAZ stainless steel				Weld zone (X_0)	HAZ carbon steel			
	X'_4	X'_3	X'_2	X'_1		X_1	X_2	X_3	X_4
mm	20	15	10	5	0	5	10	15	20

DOI 10.12776/ams.v23i4.1002 p-ISSN 1335-1532
e-ISSN 1338-1156

The weld specimens were cut from the as – welded plates with 20 x 5 x 3 mm. Metallography samples were polished and etched in 5g $FeCl_3$ + 15cm^3 HCl + 50÷100cm^3 H_2O for stainless steel and weld metal and 3% HNO_3 for carbon steel side. The microstructures and hardness test were measured by OM LEICA MDS4000M and hardness tester ARK600. X – ray (D500), FE-SEM (JSM7600F), and TEM (JEM1400 Plus) were used to determine the phases, carbides which formed in HAZ of carbon steel and austenitic stainless steel.

3 Results and discussion

3.1 Peak temperature profiles and cooling rate

Fig. 1 shows the temperature distribution profiles which measured by thermocouples in carbon steel and stainless steel sides during heating and cooling processes. The heating cycle was very fast, within 10 seconds to 40 seconds to reach the peak temperature in the melted zone and 10 mm from the fusion line respectively. During cooling cycle, the cooling rate was very high in the temperature ranged from melted point to 900^{0}C, then reduced gradually in the HAZ of the base metals. **Table. 4** presents the cooling rates measured in experiment processes that depended on temperature and positions.

The peak temperature profile in HAZ of carbon steel is displayed in **Fig. 2**. The measured values were agreement with theory calculation. The HAZ width of carbon steel was around 15 – 22 mm.

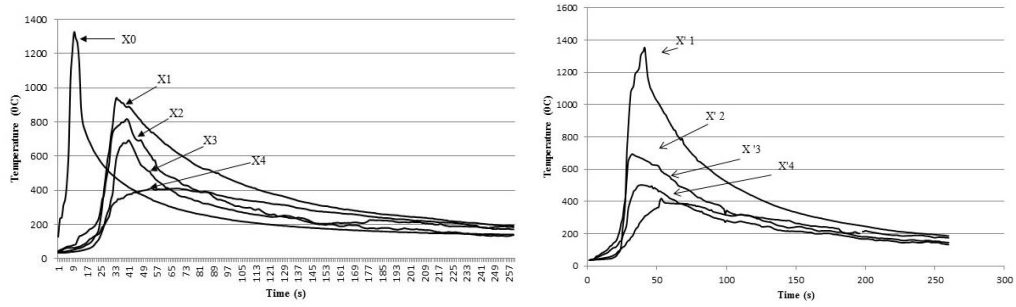

(a) Carbon steel (b) Stainless steel

Fig. 1 Measured heating and cooling profiles in HAZ

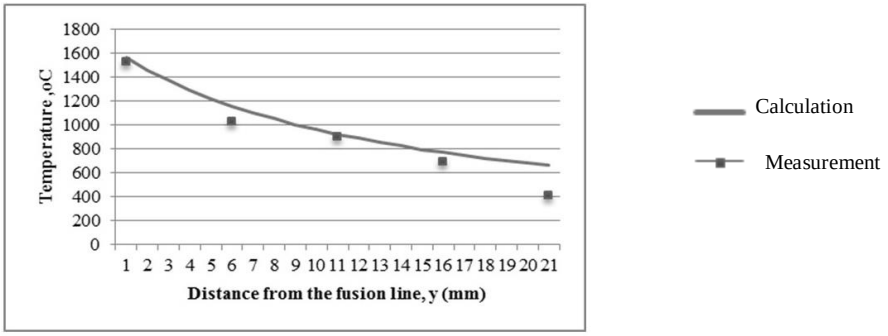

Fig. 2 The peak temperature (T_p) profile in HAZ of carbon steel

DOI 10.12776/ams.v23i4.1002 p-ISSN 1335-1532
e-ISSN 1338-1156

Table 4 Cooling rate in HAZ of carbon steel

Positions	Units	CL	5mm	10 mm	15 mm	20 mm
$T_p(^0C)$	^0C	1528	1025	903	691	411
V_{ng} (T>900^{0}C)	^0C/sec	110	40.6	-	-	-
V_{ng} (T = 900 – 500)	^0C/sec	32	16.7	15.7	-	-
V_{ng} (T<500^{0}C)	^0C/sec	1.5	1.8	1.8	1.5	1.1

In order to study the effect of cooling rate on microstructures in HAZ of the dissimilar metal weld between carbon steel and stainless steel, phases transformation can be predicted by using CCT diagrams. **Fig. 3** illustrates CCT diagrams of carbon steel and stainless steel that were measured by thermocalc software.

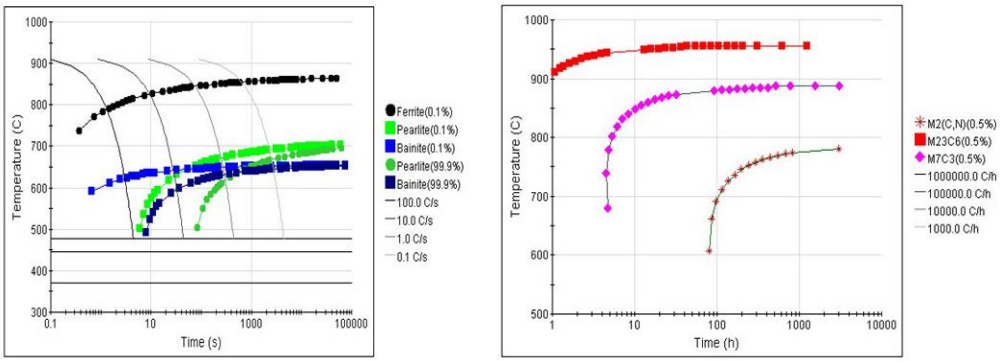

Fig. 3 CCT diagram of carbon steel and stainless steel by JmatPro

3.2 Microstructure in HAZ of carbon steel

The HAZ microstructures and grain sizes of carbon steel changed significantly from the fusion line to base metal. The average grain size near the fusion boundary was counted by 4.5 grade level, then reduced to 10.9 grade level in the base metal. Depending on cooling and peak temperature, the existed phases are varied in each zone. **Fig. 4** shows the microstructures in each separate region in HAZ of carbon steel. The high cooling rate at the fusion boundary of up to 110 ^{0}C/s caused forming the fully Martensitic layer along the fusion line. Lower cooling rates which present in **Table. 3** were measured in the experimental lead to mixed phases in others HAZ. In regions where the peak temperature is higher than A_{c3} 870^{0}C, and cooling rate is higher 2^{0}C/s, Austenitic transformed to Martensite or Bainite. Widmanstatten ferrite can be formed

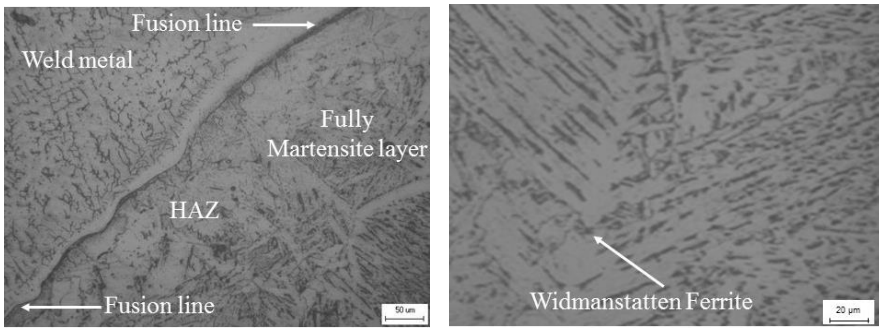

DOI 10.12776/ams.v23i4.1002 p-ISSN 1335-1532
e-ISSN 1338-1156

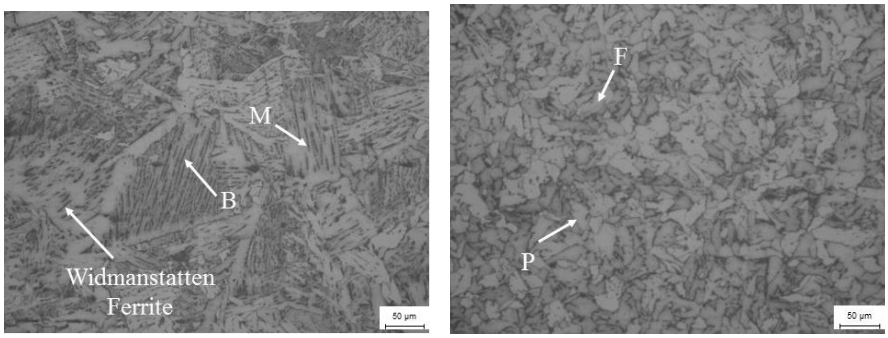

Fig. 4 Microstructure in HAZ of carbon steels. (a) – Fusion line, (b) – HAZ at 100µm, (c) –HAZ at 1200 µm from the fusion line

along grain boundaries. However, from this zone forward to base metal, the microstructures of base metal were Pearlite and Ferrite only.

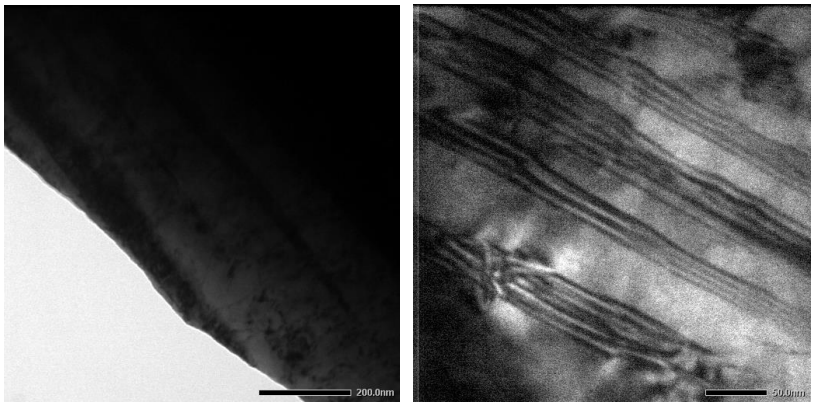

Fig. 5 Transmission electron micrograph (TEM) showing a Martensite lath and Bainitic structure in HAZ of carbon steel

3.3 Microstructure and carbide precipitation in HAZ of stainless steel

Austenite was observed in HAZ of stainless steel (**Fig. 6a**). There was not phase transformation in HAZ of stainless steel during the welding process, however, carbide precipitation can be observed in grain boundary (**Fig. 6b**). The X-ray's results show that the $Cr_{23}C_6$ located in the grain boundary while the Cr_7C_3 was in the HAZ zone of stainless steel (**Fig. 7**). The morphology of carbides $Cr_{23}C_6$ and Cr_7C_3 can be observed by TEM (Fig. 8). The CCT of stainless steel indicates that carbide $M_{23}C_6$ formed at the high temperature that ranges from 900 – 950^0C; whereas carbide M_7C_3 was precipitated at the lower temperature from 780 - 900^0C. Carbide M_2(C,N) can be found when the temperature ranges from 600 - 880^0C with low cooling rate and the retention time of the material in the sensitization temperature range is long enough for precipitation to take place. Carbide precipitation did not occur immediately next to the fusion line, it usually occurred at a short distance away from it. This phenomenon can be explained by using thermal cycle during the welding process. The material next to the fusion boundary experienced the highest peak temperature and cooling rate. Consequently, the cooling rate through the precipitation range was too high to allow carbide precipitation to occur. Consider the

DOI 10.12776/ams.v23i4.1002 p-ISSN 1335-1532
e-ISSN 1338-1156

microstructure in HAZ zone where the peak temperature was lower 600^0C, there were no signs of grain boundary precipitation.

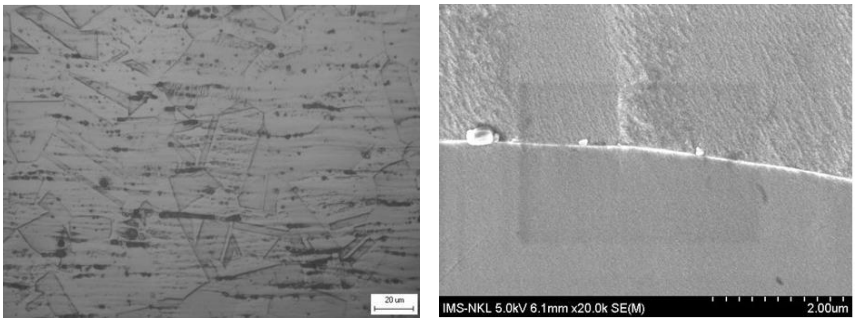

(a) (b)

Fig. 6 The microstructure in HAZ of stainless steel, (a) HAZ stainless steel, (b) Carbide precipitation at grain boundary by SEM

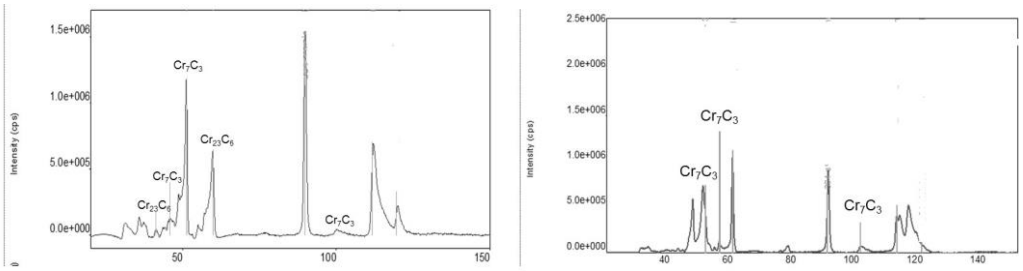

(a) (b)

Fig. 7 The X-ray's results in HAZ of stainless steel, (a) near the fusion boundary (b) HAZ

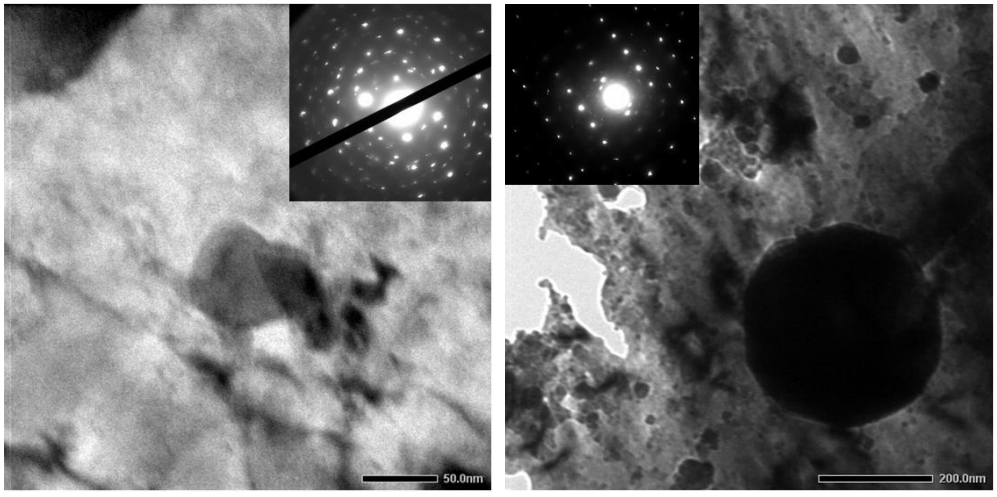

(a) (b)

Fig. 8 The TEM images in grain-boundary (a) and HAZ zone (b) of stainless steel

DOI 10.12776/ams.v23i4.1002 p-ISSN 1335-1532
e-ISSN 1338-1156

4 Conclusion

The relationship between cooling rate and microstructures in the HAZ of the dissimilar weld between carbon steel and austenitic stainless steel can be summarised:

- The changing of peak temperature and cooling rate from the fusion line to base metal caused the forming distinct phases in HAZ of carbon steel. In the cooling rate range, from 110 ^{0}C/sec at the fusion line to 1.1 ^{0}C/sec in the base metal, the microstructure changed from the fully Martensitic layer to Bainite to Pearlite. Widmanstatten Ferrite was found near the fusion boundary.
- There was not phase transformation in HAZ of stainless steel during the welding process, however, carbide precipitation can be observed in the grain boundary. Carbide $M_{23}C_6$ or M_7C_3 was found at the Austenitic grain boundary.

References

[1] A. G. Glover, J. T. McGrath, M. J. Tinkler, G. C. Weatherly: Welding Research Supplement, 1977, p. 267 - 273

[2] X. Fang et al.: Materials Science and Technology, Vol. 18, 2002, p. 47–84, DOI 10.1179/026708301125000203

[3] Bangaru, V. Narasimha – rao, A. K. Sachdev: Metallurgical Transactions A, Vol. 13A, 1982, p. 1899–1906

[4] J. C. Ion, K. E. Easterling, M. F. Ashby: Acta Metallurgica, Vol.32, 1984, Issue 11, p.1949 – 1955, DOI. 10.1016/0001-6160(84)90176-7

[5] H. Arya, K. Singh, S. Singh: International Journal on Theoretical and Applied Research in Mechanical Engineering, Vol. 2, 2013, No. 2, p. 71 – 77

[6] A. De et al.: Science and Technology of Welding and Joining, Vol. 8, 2013, No. 6, p. 319–332, DOI 10.1179/136217103225005633

[7] E. O. Aweda, I. M. Dagwa, M. Dauda, E.T. Dauda: Journal of Production Engineering, 2013, No. 2, p. 20–24

[8] J. Dutta, Narendrana, S.: Review of Industrial Engineering Letters, Vol. 1, 2014, No. 3, p. 55-66, DOI: 10.18488/journal.71/2014.1.2/71.2.55.66

[9] Rahul Kumar, Harish K Arya, Saxena RK: Material Science and Engineering, Vol. 4, 2014, ISSN: 2249-6645, p. 222 – 228

[10] A. Choubey, V. S. Jatti: Wseas Transactions on Applied and Theoretical Mechanical, Vol. 9, 2014, E – ISSN:2224 – 3429, p. 222 – 228

[11] Huei – Sen Wang: Materials Transactions, Vol. 46, 2005, No. 3, The Japan Institute of Metals, p. 593 – 601

[12] M. L. Greeff, M. du Toit: Welding Research, 2006, p. 243 – 251

[13] V. P. Kujanpaa, S. A. David and C. L. White: Welding Research Supplement, 1987, p. 222–228

[14] J. C. Lippold, W. A. Baeslack III and I. Varol: Welding Research Supplement, 1992, p. 1 – 14

[15] T. Kasuya, N. Yurioka, M. Okumura: *Methods for predicting maximum hardness of heat – affected zone and selecting necessary preheat temperature for steel welding*, Nippon Steel Technical Report, No. 65, UDC621.791.011/.02, 1995, p. 7 – 14

[16] Andrey Ivanovich Shveyov: "*Method of predicting the hardness of welded joints*", International Journal of Applied Engineering Research, ISSN 0973-4562, Vol. 11, No. 3, 2016, p. 1603 – 1608, www.ripublication.com

[17] K. Poorhaydari, B. M. Patchett, D. G. Ivey: Supplement to The Welding Journal, 2005, p. 149 – 155
[18] A. C. Nunes, JR: Welding Research Supplement, 1983, p. 165 – 170
[19] Djarot B. Darmadi: ARPN Journal of Engineering and Applied Science, ISSN 1819 – 6608, Vol. 11, No. 2, 2016, p. 790 – 795
[20] M. Grujicic et al.: Journal of Materials Engineering and Performance, Vol. 22(5), 2013, p. 1209 – 1222, DOI:10.1007/s11665-012-0402-1
[21] Sandro M M Lima e Silva et al: High Temperatures – High Pressures, Vol. 35/36, 2004, p. 117 – 126, DOI.10.1068/htjr086
[22] J. Hu, H. L. Tsai: International Journal of Heat and Mass Transfer 50, 2007, p. 833 – 846, DOI: 10.1016/j.ijheatmasstransfer.2006.08.025
[23] J. Hu, H. L. Tsai: International Journal of Heat and Mass Transfer 50, 2007, p. 808 – 820, DOI: 10.1016/j.ijheatmasstransfer.2006.08.026
[24] Sindo Kou: *Welding Metallurgy*, 2nd Edition, John Wiley & Sons, Inc., Hoboken, New Jersey, 2003
[25] J. Trzaska, A. Jagiello, L. A. Dobrzanski: Archives of Materials Science and Engineering, Vol. 39, 2009, No. 1, p. 13–20
[26] R. W. Fonda, G. Spanos: Metallurgical and Materials Transactions A, Vol. 31, 2000, No. 9, p. 2145 – 2153
[27] J. Caron et al.: Welding Journal, Vol. 89, 2010, p. 151 – 160